Research Square

Preprints are preliminary reports that have not undergone peer review.
They should not be considered conclusive, used to inform clinical practice,
or referenced by the media as validated information.

Biomimetic Apoptotic Nanovesicles Derived from T Cells Target Neuroinflammation and Enhance Neural Regeneration via TGFBR2-Mediated Signaling for Spinal Cord Injury Repair

Ziqi Zhu
Department of Spine Surgery, Shanghai East Hospital, School of Medicine, Tongji University
Beiduo Shen
Department of Spine Surgery, Shanghai East Hospital, School of Medicine, Tongji University
Tianyu Li
Clinical college of Anhui medical university
Qingyue Yuan
Department of Neurosurgery, School of Clinical Medicine of Nanjing Medical University
Da Tan
Department of Neurosurgery, Shanghai Tenth People' s Hospital, Tongji University School of Medicine
Yiyang Cheng
Department of Neurosurgery, Shanghai Tenth People' s Hospital, Tongji University School of Medicine
Wenxin Liang
Department of Neurosurgery, Shanghai Tenth People' s Hospital, Tongji University School of Medicine
Qiang Zhou
Department of Neurosurgery, Shanghai Tenth People' s Hospital, Tongji University School of Medicine
Xianzhen Chen
Department of Neurosurgery, School of Clinical Medicine of Nanjing Medical University
Mingran Luo
Department of Orthopedics, the Affiliated Hospital of Xuzhou Medical University
Xie Tao
todxietao@163.com

Department of Orthopedic Surgery, Affiliated Hangzhou First People's Hospital, Westlake University, School of Medicine

---

Research Article

Keywords: apoptotic nanovesicles, spinal cord injury, neuroregeneration, immunomodulation, transforming growth factor-β receptor 2

Posted Date: April 9th, 2026

DOI: https://doi.org/10.21203/rs.3.rs-9240762/v1

License: This work is licensed under a Creative Commons Attribution 4.0 International License. Read Full License

Additional Declarations: No competing interests reported.

Abstract

Spinal cord injury (SCI) remains a major clinical challenge because persistent neuroinflammation and limited intrinsic regeneration jointly impede functional recovery. Here, biomimetic apoptotic nanovesicles (Apo-nanovesicles) derived from early apoptotic Jurkat T cells are developed as a cell-free nanotherapeutic platform for SCI repair. The Apo-nanovesicles retain apoptosis-associated membrane cues, including phosphatidylserine, while exhibiting uniform nanoscale size, favorable colloidal stability, and good biocompatibility. In vitro, they are efficiently internalized by microglia, suppress pro-inflammatory activation, and promote a reparative phenotype. They also enhance neuronal differentiation of neural stem cells while reducing astroglial commitment. In a murine SCI model, Apo-nanovesicle treatment significantly improves locomotor recovery, attenuates glial scar formation, and establishes a regenerative lesion microenvironment. Transcriptomic profiling identifies TGF-β signaling as a major pathway associated with treatment response, and network analysis together with experimental validation reveals transforming growth factor-β receptor 2 (TGFBR2) as a central regulatory node. These findings indicate that Apo-nanovesicles promote SCI repair by coupling inflammatory resolution with neural regeneration through TGFBR2-mediated signaling. This work establishes apoptosis-mimetic nanovesicles as a promising biomimetic strategy for neuroregenerative therapy.

Introduction

Spinal cord injury (SCI) remains one of the most formidable challenges in neurological medicine, with an estimated annual incidence of 250,000-500,000 cases worldwide and often devastating consequences for the quality of life of patients. [1,2] The pathophysiology of SCI involves a complex cascade of events beginning with the primary mechanical insult followed by a secondary injury phase characterized by inflammation, oxidative stress, mitochondrial dysfunction, and glial scar formation that collectively inhibit neural regeneration and functional recovery. [3,4] Despite decades of research, effective therapeutic options remain limited. Early surgical decompression is currently the most effective intervention, while pharmacological approaches such as methylprednisolone remain controversial despite their widespread use. [5] This therapeutic impasse has motivated the exploration of innovative strategies ranging from stem cell therapy and biomaterial scaffolds to neuromodulation techniques.

In recent years, the field of regenerative medicine has witnessed growing interest in cell-derived nanotherapeutics as a promising alternative to cell-based therapies. [6-8] Among these, extracellular vesicles (EVs) have emerged as important mediators of intercellular communication with demonstrated potential in modulating immune responses and promoting tissue repair. [9,10] However, conventional EVs derived from mesenchymal stem cells or other sources face challenges related to scalable production, functional heterogeneity, and limited targeting specificity. [11,12] Meanwhile, the immunomodulatory properties of apoptotic cells and their derivatives have gained increasing attention. During programmed cell death, apoptotic cells release "find-me" and "eat-me" signals that actively suppress inflammatory responses and promote tissue homeostasis. [13-15] This intrinsic biological

property suggests that biomimetic strategies harnessing apoptotic mechanisms may offer novel therapeutic opportunities for inflammatory conditions such as SCI.

The investigation of apoptosis-derived vesicles represents an emerging frontier in nanomedicine. Apoptotic bodies (1-5 μm), the largest vesicles shed during programmed cell death, were initially considered merely cellular debris but are now recognized as key players in immunomodulation and tissue regeneration. [16] However, the translational progress of natural apoptotic bodies is significantly constrained by inherent biological and manufacturing challenges, such as limited and inconsistent yields, intrinsically heterogeneous molecular compositions, and insufficient purification, all of which fundamentally restrict standardized production and reliable therapeutic reproducibility. [17-20]

Recent efforts have focused on nanovesicles derived from apoptotic membranes that retain key biological signaling molecules while exhibiting improved physicochemical controllability and biodistribution. [21] Notably, studies have demonstrated that nanovesicles derived from apoptotic cell membranes exhibit particularly potent immunoregulatory functions, owing to preserved surface expression of phosphatidylserine (PS) and other apoptosis-associated molecular patterns. [22,23] A significant gap remains in our understanding of how apoptotic membrane-derived nanovesicles interact with the central nervous system (CNS) microenvironment. This is particularly relevant for SCI, where excessive inflammation and impaired regeneration represent critical therapeutic targets.

In this study, we developed biomimetic nanovesicles derived from staurosporine-induced early apoptotic Jurkat T cells membrane (Apo-nanovesicles). T cells were selected as the cellular source due to their well-documented immunomodulatory properties and inherent capacity to target inflammatory sites—a trait potentially transferable to derived vesicles. Our approach combines differential centrifugation and sequential extrusion techniques to generate nanovesicles that retain key apoptotic surface biomarkers, particularly phosphatidylserine, while exhibiting uniform size distribution and excellent colloidal stability. We conducted a comprehensive evaluation of the therapeutic potential of Apo-nanovesicles through integrated in vitro and in vivo approaches. Our investigation revealed their ability to redirect microglial polarization toward an anti-inflammatory M2 phenotype, enhance the neuronal differentiation of neural stem cells while inhibiting astrogliosis, and promote functional recovery in SCI mice. Through transcriptomic analysis, we further elucidated that these therapeutic effects were mediated through specific activation of transforming growth factor-β receptor 2 (TGFBR2), the key receptor in the TGF-β signaling pathway. By leveraging the innate biological properties of apoptotic T cells and engineering them into well-characterized nanovesicles, we have developed a promising cell-free therapeutic strategy with significant translational potential for SCI.

Experimental Section

Generation of Apo-Nanovesicles from Early Apoptotic T Cells

Jurkat Clone E6-1 human T lymphocytes were cultured in RPMI 1640 medium supplemented with 10% fetal bovine serum and 1% penicillin–streptomycin under humidified conditions (37 °C, 5% CO_2). To enrich the early apoptotic population, cells were exposed to staurosporine (0.5 μM) for 12 h. Following treatment, the cells were collected by centrifugation (200 × g, 10 min), rinsed twice with ice-cold phosphate-buffered saline (PBS), and resuspended in hypotonic TM buffer composed of 10 mM Tris-HCl, 10 mM $MgCl_2$, and a protease inhibitor cocktail. The suspension was held at 4 °C overnight to facilitate osmotic swelling. Mechanical disruption was then performed using a glass Dounce homogenizer with 20 complete strokes. Unbroken cells, nuclei, and large debris were removed by two sequential centrifugation steps at 3,000 × g for 10 min. The resulting post-nuclear supernatant was ultracentrifuged at 100,000 × g for 45 min at 4 °C to harvest membrane fractions. The membrane pellet was washed once with PBS, re-collected by ultracentrifugation, and quantified with a bicinchoninic acid assay prior to storage at −80 °C. Control nanovesicles were generated in parallel from non-apoptotic Jurkat cells using the same membrane-isolation procedure. Apo-nanovesicles were subsequently fabricated by serial extrusion of the isolated apoptotic membrane through 1000, 400, and 200 nm polycarbonate membranes using a mini-extruder, with more than 15 passes at each pore size to ensure uniform nanoscale reformulation.

The morphology of the vesicles was examined using a transmission electron microscope (HT7800 series, Hitachi High-Tech, Japan). Particle size distribution and particle concentration were determined by nanoparticle tracking analysis using a ZetaView system (Particle Metrix, Germany). Hydrodynamic diameter, polydispersity index, and zeta potential were measured on a Zetasizer Pro instrument (Malvern Panalytical, UK). The apoptotic status of parental Jurkat cells and the preservation of phosphatidylserine on Apo-nanovesicles were assessed using a FITC Annexin V/propidium iodide apoptosis detection kit, followed by confocal fluorescence imaging and flow-cytometric quantification.

Expansion and Maintenance of Mouse Neural Stem Cells

Mouse neural stem cells (mNSCs) were obtained from a commercial supplier and expanded as free-floating neurospheres in serum-free DMEM/F12-based medium supplemented with N-2, B-27, recombinant murine epidermal growth factor (EGF, 20 ng mL^{-1}), and recombinant murine basic fibroblast growth factor (bFGF, 20 ng mL^{-1}). Cultures were maintained at 37 °C in a 5% CO_2 incubator, and medium was replenished every 2–3 days. For routine passaging, neurospheres were collected by gentle centrifugation, dissociated into single cells using Accutase, and re-seeded at the desired density. The stem-like phenotype of the cultures was confirmed by the expression of canonical neural stem cell markers in subsequent immunostaining experiments.

Cytocompatibility Assessment of Apo-Nanovesicles toward mNSCs

To evaluate the biosafety of Apo-nanovesicles, mNSCs were seeded in 24-well plates at 1 × 10^5 cells per well and incubated with the indicated formulations for 72 h. Cell viability was first visualized using a

LIVE/DEAD fluorescence assay based on calcein AM and ethidium homodimer-1 staining. Images were acquired under identical exposure settings and analyzed using ImageJ to determine the fraction of viable cells. In parallel, metabolic activity was quantified using a Cell Counting Kit-8 (CCK-8) assay. Briefly, mNSCs were plated in 96-well plates at 5 × 10^3 cells per well, treated for 72 h, incubated with CCK-8 reagent for 2 h at 37 °C, and the absorbance at 450 nm was recorded using a microplate reader.

EdU-Based Proliferation Analysis

For proliferation analysis, mNSCs were exposed to Apo-nanovesicles or control formulations under standard proliferative culture conditions for 72 h. Cells were then pulsed with 5-ethynyl-2'-deoxyuridine (EdU, 10 μM) for 4 h, fixed with 4% paraformaldehyde, permeabilized with 0.1% Triton X-100, and processed according to the manufacturer's protocol for click-chemistry-based detection. Nuclei were counterstained with DAPI, and the proportion of EdU-positive cells was determined from randomly selected microscopic fields.

Cellular Internalization of Apo-Nanovesicles

The uptake of Apo-nanovesicles by microglia was examined using SIM-A9 cells. Cells were maintained in DMEM/F12 containing 10% fetal bovine serum and 1% penicillin–streptomycin and seeded onto glass-bottom dishes before treatment. Apo-nanovesicles were labeled with the lipophilic tracer DiD and incubated with SIM-A9 cells at 37 °C. After incubation, the cells were washed thoroughly with PBS to remove unbound vesicles, fixed with 4% paraformaldehyde, and stained with phalloidin for F-actin visualization and DAPI for nuclear counterstaining. Intracellular fluorescence was recorded by confocal microscopy. For quantitative analysis, treated cells were harvested and analyzed by flow cytometry, and the mean fluorescence intensity was calculated using FlowJo software.

RNA Isolation and Quantitative Real-Time PCR

Total RNA from cultured cells or spinal cord tissues was isolated with TRIzol reagent following the manufacturer's protocol. RNA concentration and purity were determined using a NanoDrop One microvolume spectrophotometer. Equal amounts of RNA (500 ng per reaction) were reverse-transcribed into cDNA using a reverse transcription kit suitable for real-time PCR. Quantitative PCR was performed using an intercalating-dye-based master mix on a CFX96 Touch real-time PCR platform. Relative gene expression was calculated using the 2^−ΔΔCt method with *Gapdh* as the internal reference gene unless otherwise specified. Primer sequences are provided in Table S1.

Immunofluorescence Staining of Cultured Cells and Spinal Cord Sections

Cultured cells were fixed in freshly prepared 4% paraformaldehyde, permeabilized with 0.1% Triton X-100, and blocked in 5% normal donkey serum for 1 h at room temperature. Samples were then incubated with primary antibodies overnight at 4 °C, washed extensively, and incubated with species-matched fluorophore-conjugated secondary antibodies for 1 h at room temperature. Nuclei were counterstained with DAPI. For F-actin visualization, phalloidin-based fluorescent probes were used where appropriate. Images were acquired using a confocal microscope under identical detector settings for each comparison group.

For tissue immunostaining, mice were deeply anesthetized and transcardially perfused with PBS followed by 4% paraformaldehyde. Spinal cord segments encompassing the lesion epicenter were harvested, post-fixed overnight, cryoprotected in 30% sucrose, embedded in OCT compound, and sectioned at 10 μm using a cryostat. Frozen sections were permeabilized with 0.25% Triton X-100, blocked with serum-containing buffer, and processed with the same primary/secondary antibody workflow described above. Fluorescence intensity was quantified from matched anatomical levels and normalized to the control group where indicated.

Primary antibodies against SOX2, NESTIN, TUJ1, TNF-α, IL-10, NEUN, GFAP, IBA1, TGFBR2, phospho-SMAD2, and SMAD4 were obtained from established commercial vendors, including Cell Signaling Technology (USA), Abcam (UK), Merck Millipore (USA), and FUJIFILM Wako (Japan).

In Vitro Microglial Inflammation Model

To model the inflammatory microenvironment associated with spinal cord injury, SIM-A9 microglia were seeded in 24-well plates at 1×10^5 cells per well and allowed to adhere overnight. Cells were then challenged with lipopolysaccharide (LPS, 100 ng mL^{-1}) for 12 h to induce pro-inflammatory activation. Apo-nanovesicles or control nanovesicles were subsequently added, and the cells were cultured for an additional 24 h. RNA and protein samples were collected for RT-qPCR and immunofluorescence analyses of M1/M2-associated markers.

Mouse Model of Spinal Cord Injury and In Vivo Treatment

Female C57BL/6J mice (8 weeks old, 18–20 g) were used for all in vivo studies. Anesthesia was induced and maintained with 2% chloral hydrate. After a midline dorsal incision and paravertebral muscle dissection, a laminectomy was performed at the T9 vertebral level to expose the spinal cord. A standardized contusive injury was created by compressing the cord with calibrated forceps mounted on a stereotaxic apparatus for 5 s. Mice received routine postoperative care, including thermal support, analgesia when required by institutional policy, and manual bladder expression twice daily until spontaneous voiding resumed. Apo-nanovesicles or control formulations were administered according to the experimental design, and locomotor recovery was monitored longitudinally using the Basso Mouse Scale.

RNA-seq

For RNA-seq analysis, a 1 cm segment of spinal cord tissue centered on the lesion site was rapidly dissected on ice and homogenized in TRIzol reagent. RNA integrity and fragment distribution were assessed using a currently marketed automated electrophoresis platform (4150 TapeStation, Agilent Technologies, USA). Libraries were prepared using the NEBNext Ultra II RNA Library Prep workflow for Illumina-compatible sequencing. Sequencing was performed on an Illumina platform, and downstream analyses were carried out using standard bioinformatics pipelines for differential expression, enrichment analysis, gene set enrichment analysis, and protein–protein interaction network construction.

Statistical Analysis

All data are presented as mean ± standard deviation (SD), as indicated in the figure legends. Statistical analyses were performed using GraphPad Prism 10.0. Comparisons between two groups were analyzed using a two-tailed unpaired Student's t-test. For comparisons involving three or more groups, one-way or two-way analysis of variance (ANOVA) followed by Tukey's multiple-comparison test was applied as appropriate. A value of $p < 0.05$ was considered statistically significant.

Results & Discussion

Apo-Nanovesicles Preserve Apoptotic Membrane Cues while Maintaining Favorable Nanoscale Characteristics

To engineer a biomimetic nanotherapeutic platform with targeted immunomodulatory and regenerative functions, Apo-nanovesicles were fabricated from early apoptotic Jurkat T cells. The selection of Jurkat T cells was motivated by their intrinsic immunoregulatory properties and their natural tropism toward inflammatory microenvironment—features anticipated to be preserved in the derived vesicles. [24] Apoptosis was efficiently induced via staurosporine treatment, a well-established apoptosis trigger. [25] Flow-cytometric analysis using Annexin V/PI staining demonstrated efficient enrichment of an Annexin V^+/PI^- population after staurosporine treatment (Figure 1A), and fluorescence imaging further confirmed robust phosphatidylserine externalization on the cell surface (Figure 1B).

Apo-nanovesicles were prepared through a multi-step process involving hypotonic lysis, mechanical homogenization, differential centrifugation, and sequential extrusion through polycarbonate membranes with progressively smaller pore sizes. TEM revealed that both control nanovesicles and Apo-nanovesicles exhibited spherical, bilayer morphologies smiliar to natural extracellular vesicles (Figure 1C). Flow cytometric evaluation demonstrated that over 90% of Apo-nanovesicles were Annexin V^+/PI^-, confirming the preservation of apoptosis-specific membrane components, particularly PS (Figure 1D). This finding was further validated by fluorescence staining (Figure 1E).

NTA indicated that Apo-nanovesicles possessed a narrow size distribution with a mean hydrodynamic diameter of approximately 130 nm, comparable to that of control nanovesicles (Figure S1, Supporting Information). Notably, Apo-nanovesicles exhibited a significantly lower zeta potential than control nanovesicles (Figure 1F), consistent with the enhanced surface negativity characteristic of apoptotic membranes due to PS externalization. [26] This result affirms the successful retention of apoptotic membrane properties in the engineered vesicles. DLS measurements confirmed that both vesicle types maintained excellent colloidal stability over 7 days at 4 °C, with no significant change in size distribution (Figure 1G) and polydispersity indices (PDI) consistently below 0.3 (Figure 1H), indicating their suitability for therapeutic applications. Collectively, these data demonstrate the successful fabrication of Apo-nanovesicles that not only mimic the physical characteristics of natural vesicles but also retain key apoptotic signaling molecules, positioning them as a promising biomimetic platform for modulating neuroinflammatory and regenerative processes in spinal cord injury.

Apo-Nanovesicles Reprogram Microglia toward a Reparative Phenotype

Microglia, as the resident immune cells of the central nervous system, play pivotal roles in orchestrating neuroinflammatory responses following spinal cord injury. [27] To assess the immunomodulatory potential of Apo-nanovesicles, we first evaluated their impact on microglial viability. Cytotoxicity evaluation confirmed that neither nanovesicles nor Apo-nanovesicles elicited significant cytotoxicity in SIM-A9 microglial cells (Figure 2D) establishing a favorable biosafety profile for subsequent functional assays. The live/dead viability assay revealed insignificant cytotoxicity upon Apo-nanovesicles treatment compared to control (Fig. 2C).

We next investigated the cellular internalization of Apo-nanovesicles by microglia. Confocal laser scanning microscopy and flow cytometric analysis revealed significantly enhanced uptake of DiD-labeled Apo-nanovesicles compared to control nanovesicles (Figure 2A, B) This preferential internalization is likely facilitated by the surface exposure of phosphatidylserine—a canonical "eat-me" signal that promotes phagocytic clearance by immune cells including microglia.

Under lipopolysaccharide-induced inflammatory conditions, Apo-nanovesicles demonstrated remarkable efficacy in reprogramming microglial polarization toward an anti-inflammatory phenotype. Quantitative PCR analysis showed significant downregulation of pro-inflammatory M1 markers (*Tnf-α, Il-1β*) and concurrent upregulation of M2-associated genes (*Tgf-β, Il-10*) in Apo-nanovesicles-treated groups compared to both LPS-stimulated controls and nanovesicles-treated cells (Figure 2E). This polarization shift was further validated at the protein level through immunofluorescence staining, which demonstrated attenuated TNF-α expression and enhanced IL-10 production in Apo-nanovesicles-treated microglia (Figure 2F, G).

The superior immunomodulatory performance of Apo-nanovesicles over conventional nanovesicles can be attributed to their inherited apoptotic membrane composition. Beyond phosphatidylserine, Apo-

nanovesicles preserve other critical immunomodulatory molecules—including ICAM-3 and annexin I—which may act synergistically to engage anti-inflammatory signaling pathways. [22] Additionally, Apo-nanovesicles may function as molecular decoys for pro-inflammatory cytokines through membrane-bound receptors, thereby effectively dampening neuroinflammatory cascades. [28] These findings collectively demonstrate that Apo-nanovesicles serve as potent nanoscale immunomodulators capable of redirecting microglial polarization toward a reparative phenotype in inflammatory microenvironments. This capacity to mitigate neuroinflammation while promoting tissue-repairing immune responses positions Apo-nanovesicles as a promising therapeutic candidate for controlling pathological inflammation in CNS disorders.

Apo-nanovesicles Enhance Neuronal Differentiation of Neural Stem Cells

The capacity to direct NSCs fate toward neuronal lineage while minimizing astrocytic differentiation represents a critical therapeutic objective for spinal cord repair. To evaluate the influence of Apo-nanovesicles on NSCs behavior, we first investigated their biocompatibility and cellular uptake. Under proliferative conditions, mNSCs formed characteristic neurospheres (Figure 3A) and exhibited robust expression of stemness markers, including nuclear SOX2 and cytoplasmic NESTIN, confirming their undifferentiated state (Figure 3B). Both nanovesicles and Apo-nanovesicles were efficiently internalized by mNSCs (Figure 3H, S2), indicating favorable cellular interactions. Viability assessments, utilizing both Live/Dead staining and CCK-8 assays, confirmed that neither vesicle type induced significant cytotoxicity after 72 h of exposure (Figure 3C–E). Moreover, EdU incorporation assays revealed that treatment with Apo-nanovesicles did not impair NSCs proliferative capacity (Figure 3F, G), collectively affirming their excellent biocompatibility and suitability for neural applications.

We next investigated the ability of Apo-nanovesicles to influence NSCs lineage commitment under differentiation-promoting conditions. Remarkably, mNSCs treated with Apo-nanovesicles exhibited a pronounced shift toward neuronal lineage, as evidenced by significant transcriptional upregulation of early and mature neuronal markers, including *Tuj1, Map2, NeuN,* and *Dcx* (Figure 4B–E). Concurrently, a substantial downregulation of the astrocytic marker *Gfap* was observed at the mRNA level (Figure 4H). Immunofluorescence analysis further corroborated these findings, demonstrating a marked increase in $TUJ1^+$ and $NEUN^+$ cells, alongside a significant reduction in $GFAP^+$ astrocytes, in the Apo-nanovesicles-treated group compared to both untreated and nanovesicles-treated controls (Figure 4F, G, I, J).

Notably, Apo-nanovesicles consistently outperformed conventional nanovesicles in promoting neuronal commitment and suppressing glial differentiation, suggesting that the unique function inherited from the apoptotic T-cell membrane actively instructs neurogenic programming. The presence of specific apoptosis-associated signals, such as phosphatidylserine, may engage receptors on NSCs that bias differentiation toward neuronal fates, potentially through the activation of pro-neurogenic signaling pathways. This capacity to favorably promote NSCs differentiation—enhancing neurogenesis while

concurrently mitigating astrogliosis—highlights the regenerative utility of Apo-nanovesicles. By creating a microenvironment conducive to neuronal generation, Apo-nanovesicles present a compelling cell-free strategy for overcoming the limited intrinsic regenerative capacity of the injured spinal cord.

Apo-Nanovesicles Improve the Lesion Microenvironment and Promote Functional Recovery after SCI

Building upon the compelling in vitro evidence demonstrating their immunomodulatory and pro-neurogenic capabilities, we next sought to evaluate the therapeutic potential of Apo-nanovesicles in a murine model of SCI. Functional recovery of hindlimb locomotion was systematically monitored over an 8-week period using the Basso Mouse Scale (BMS), a sensitive and validated metric for assessing open-field locomotion in mice. Animals treated with Apo-nanovesicles exhibited a markedly accelerated and superior recovery compared to those in both the SCI control group and the conventional nanovesicles-treated group (Figure 5A). The significant improvement in BMS scores, evident from the early phases of the recovery process and sustained throughout the observational period, underscores the potent and durable therapeutic impact of Apo-nanovesicles administration.

To corroborate the therapeutic efficacy observed in behavioral analyses, we performed comprehensive immunofluorescence staining and qPCR analyses on spinal cord tissues harvested from the lesion. Our results unequivocally demonstrated that Apo-nanovesicles treatment fostered a pro-regenerative immune microenvironment conducive to SCI repair. Transcriptional analysis via RT-qPCR revealed a significant downregulation of the microglial marker *Iba1* alongside classic M1 phenotype-associated genes (*Tnf-α, iNOS*). This was accompanied by a concerted upregulation of key M2 anti-inflammatory cytokines (*Arg-1, Il-10*) in the Apo-nanovesicles-treated group (Figure 5B, C). This robust polarization shift was further corroborated at the protein level, as evidenced by a marked reduction in $IBA1^+$ fluorescence signals (Figure 5D, F) and a distinct phenotypic transition characterized by attenuated TNF-α and enhanced IL-10 levels within the lesion microenvironment (Figure 5E, F). The successful reprogramming of microglia toward a pro-regenerative phenotype establishes a critical immunomodulatory foundation that is indispensable for facilitating subsequent neural repair processes.

Concomitantly, Apo-nanovesicles treatment orchestrated a microenvironment highly favorable for neural regeneration. qPCR revealed a significant upregulation of key neuronal markers, including *Tuj1, Map2,* and *NeuN* (Figure 6A–C), coupled with a significant suppression of *Gfap* mRNA expression (Figure 6D), strongly indicating enhanced neuronal differentiation and attenuated astrogliosis. This transcriptional signature was robustly validated at the protein level. Immunofluorescence analysis confirmed a substantial increase in $NEUN^+$ mature neurons within the lesion area (Figure 6E, G), suggesting enhanced neuronal differentiation. Furthermore, critical assessment of glial scar formation—a major physicochemical barrier to axonal regeneration—demonstrated a pronounced attenuation of $GFAP^+$ reactive astrocytes in the Apo-nanovesicles group compared to the SCI control (Figure 6F, G). Collectively, these in vivo findings demonstrate that Apo-nanovesicles administration post-SCI

orchestrates a reparative response, encompassing a shift in microglial polarization toward an anti-inflammatory phenotype, promotion of neurogenesis, and significant attenuation of glial scar formation. These therapeutic effects creates a suitable microenvironment that ultimately facilitates substantial and sustained functional recovery after SCI.

Activation of TGFBR2 Mediates Apo-Nanovesicles-Induced Repair after Spinal Cord Injury

To elucidate the mechanistic underpinnings of the recovery promoted by Apo-nanovesicles, RNA sequencing was conducted on spinal cord tissues harvested from experimental groups. Transcriptomic profiling revealed substantial differential gene expression across groups (Fig. 7A). Enrichment analyses based on the KEGG database highlighted significant involvement of the TGF-β signaling pathway, MAPK signaling, PI3K-Akt signaling, Regulation of the actin cytoskeleton, and Focal adhesion (Fig. 7B). Gene Ontology (GO) terms further associated these differentially expressed genes with biological processes such as neuron differentiation, cell differentiation, nervous system development, axonogenesis, and synaptic organization (Fig. 7C). Gene Set Enrichment Analysis (GSEA) corroborated these findings, showing coordinated upregulation of gene sets related to the TGF-β pathway following Apo-nanovesicles treatment (Fig. 7D). Protein-protein interaction (PPI) network analysis identified TGFBR2 as a central hub within the regulatory network, suggesting its pivotal role in mediating the therapeutic benefits of Apo-nanovesicles (Fig. 7E). Subsequent qPCR and immunofluorescence validation confirmed the upregulation of TGFBR2, p-SMAD2 and SMAD4 expression in Apo-nanovesicles-treated SCI mice (Fig. 7F-H, S3).

Mechanistically, our data suggest that Apo-nanovesicles do not merely attenuate inflammation in a passive manner, but instead engage a TGFBR2-centered pro-repair signaling axis. Canonical TGF-β signaling is initiated by ligand engagement of TGFBR2, followed by recruitment and phosphorylation of TGFBR1 and subsequent activation of SMAD2/3–SMAD4 transcriptional complexes, while parallel non-canonical modules such as PI3K–Akt and MAPK provide context-dependent amplification. [29,30] In the injured spinal cord, such signaling is profoundly cell-state- and niche-dependent. Recent studies have shown that microglia are indispensable coordinators of SCI repair, orchestrating communication with astrocytes and infiltrating leukocytes to limit secondary damage and support tissue preservation. [31] In parallel, fibrotic scar formation is now recognized as a heterogeneous process, in which discrete fibroblast subsets can either exacerbate matrix deposition or contribute to angiogenic remodeling, underscoring that regenerative benefit depends on selective reprogramming, rather than indiscriminate pathway activation. [32] Within this framework, the elevated TGFBR2 signaling observed here likely reflects a beneficial rebalancing of the lesion microenvironment, whereby Apo-nanovesicles bias microglia toward a pro-resolving phenotype, restrain maladaptive gliosis, and increase permissiveness for axonal extension and neuronal maturation. This interpretation is further aligned with recent studies showing that extracellular-vesicle-based or bioelectrically instructive platforms can improve SCI repair by enhancing M2-like immune polarization, suppressing oxidative injury, accelerating neuronal differentiation, and promoting functional recovery. [33-36] Collectively, these findings support that Apo-nanovesicles act upstream of a TGFBR2-dominant molecular program that integrates neuroimmune

modulation with neural regeneration, ultimately enabling structural repair and sustained locomotor recovery after SCI.

Conclusion

In summary, biomimetic Apo-nanovesicles derived from early apoptotic Jurkat T cells are developed as a cell-free therapeutic platform for spinal cord injury repair. By preserving apoptosis-associated membrane signals, these nanovesicles effectively modulate the post-injury microenvironment, promote anti-inflammatory microglial polarization, enhance neuronal differentiation of neural stem cells, and suppress astrogliosis. These coordinated effects translate into reduced glial scar formation and improved functional recovery in vivo. Mechanistically, transcriptomic and validation analyses identify TGFBR2-centered TGF-β signaling as a key pathway linking immunomodulation to neural regeneration. This study not only highlights the therapeutic value of apoptosis-mimetic nanovesicles in SCI, but also expands the design space of biomimetic nanomedicine for neuroinflammatory and neurodegenerative disorders.

Declarations

Acknowledgements

Not applicable.

Credit author statement

Ziqi Zhu: Writing – original draft, Visualization, Methodology, Investigation, Formal analysis, Data curation, Conceptualization. Beiduo Shen: Methodology, Investigation, Formal analysis, Data curation. Tianyu Li: Software, Resources, Formal analysis, Data curation. Qingyue Yuan: Resources, Methodology, Investigation, Formal analysis. Da Tan: Supervision, Software, Resources. Yiyang Cheng: Validation, Supervision, Funding acquisition. Wenxin Liang: Supervision. Xianzhen Chen: Supervision. Mingran Luo: Investigation, Formal analysis, Data curation. Mingran Luo, Qiang Zhou: Supervision, Funding acquisition. Xie Tao: Resources, Project administration, Funding acquisition.

Funding

This work was financially supported by Natural Science Foundation (Grant No.XWKYHT20250097，Grant No. 2025203015).

Data availability

All data are available from the corresponding authors upon reasonable request.

Ethics approval and consent to participate

All animal procedures were approved by the Animal Ethics Committee of Tongji University (DWSB-2025232) and conducted in accordance with the NIH Guide for the Care and Use of Laboratory Animals.

Consent for publication

All authors of this study agreed to publish.

Competing interests

No potential conflicts of interest relevant to this article were reported.

Author details

[1] Department of Spine Surgery, Shanghai East Hospital, School of Medicine, Tongji University, Shanghai, 200092, China.

[2] Department of Orthopedic Surgery, Affiliated Hangzhou First People's Hospital, Westlake University School of Medicine, Hangzhou, China.

[3] Department of Orthopedics, the Affiliated Hospital of Xuzhou Medical University, Xuzhou, 221000, China.

[4] Department of Neurosurgery, School of Clinical Medicine of Nanjing Medical University, Nanjing 211166, Jiangsu, China.

[5] Department of Neurosurgery, Shanghai Tenth People' s Hospital, Tongji University School of Medicine, Shanghai 200000, China.

[6] Clinical college of Anhui medical university, Hefei, 230031, China.

References

1. M. V. Sofroniew, Dissecting spinal cord regeneration, Nature 557 (7705) (2018) 343–350.
2. C. Hamlet, L. Fauci, J. R. Morgan, E. D. Tytell, Proprioceptive feedback amplification restores effective locomotion in a neuromechanical model of lampreys with spinal injuries, Proc. Natl. Acad. Sci. U. S. A. 120 (11) (2023) e2213302120.
3. A. P. Tran, P. M. Warren, J. Silver, The biology of regeneration failure and success after spinal cord injury, Physiol. Rev. 98 (2) (2018) 881–917.

4. M. A. Anderson, J. E. Burda, Y. Ren, Y. Ao, T. M. O'Shea, R. Kawaguchi, G. Coppola, B. S. Khakh, T. J. Deming, M. V. Sofroniew, Astrocyte scar formation aids central nervous system axon regeneration, Nature 532 (7598) (2016) 195–200.
5. B. Bai, R. Zhang, C. Zhang, Y. Liu, S. Liu, C. Zou, L. Jiang, Z. Qi, X. Song, C. Li, Z. Li, K. Wu, Y. Song, M. Hou, C. Li, G. Zhou, X. Kong, D. Lei, H. Zhou, S. Feng, Spinal cord-like scaffold with rapid tissue integration enhanced spinal cord nerve repair, Adv. Mater. (2025) e05402.
6. W. Li, H. Zhang, L. Chen, C. Huang, Z. Jiang, H. Zhou, X. Zhu, X. Liu, Z. Zheng, Q. Yu, Y. He, Y. Gao, J. Ma, L. Yang, Cell membrane-derived nanovesicles as extracellular vesicle-mimetics in wound healing, Mater. Today Bio 31 (2025) 101595.
7. J. Huang, J. Zhang, J. Xiong, S. Sun, J. Xia, L. Yang, Y. Liang, Stem cell-derived nanovesicles: A novel cell-free therapy for wound healing, Stem Cells Int. 2021 (2021) 1285087.
8. A. I. Abid, G. Conzatti, F. Toti, N. Anton, T. Vandamme, Mesenchymal stem cell-derived exosomes as cell free nanotherapeutics and nanocarriers, Nanomedicine-Uk 61 (2024) 102769.
9. N. Mukerjee, H. M. Alharbi, S. Maitra, K. Anand, N. Thorat, S. Gorai, Exosomes in liquid biopsy and oncology: Nanotechnological interplay and the quest to overcome cancer drug resistance, J Liq Biopsy 3 (2024) 100134.
10. M. Kou, L. Huang, J. Yang, Z. Chiang, S. Chen, J. Liu, L. Guo, X. Zhang, X. Zhou, X. Xu, X. Yan, Y. Wang, J. Zhang, A. Xu, H. F. Tse, Q. Lian, Mesenchymal stem cell-derived extracellular vesicles for immunomodulation and regeneration: A next generation therapeutic tool?, Cell Death Dis. 13 (7) (2022) 580.
11. G. Xu, J. Jin, Z. Fu, G. Wang, X. Lei, J. Xu, J. Wang, Extracellular vesicle-based drug overview: Research landscape, quality control and nonclinical evaluation strategies, Signal transduction and targeted therapy 10 (1) (2025) 255.
12. K. Adlerz, D. Patel, J. Rowley, K. Ng, T. Ahsan, Strategies for scalable manufacturing and translation of msc-derived extracellular vesicles, Stem Cell Res 48 (2020) 101978.
13. Y. You, J. Xu, Y. Liu, H. Li, L. Xie, C. Ma, Y. Sun, S. Tong, K. Liang, S. Zhou, F. Ma, Q. Song, W. Xiao, K. Fu, C. Dai, S. Li, J. Lei, Q. Mei, X. Gao, J. Chen, Tailored apoptotic vesicle delivery platform for inflammatory regulation and tissue repair to ameliorate ischemic stroke, ACS nano 17 (9) (2023) 8646–8662.
14. P. Shi, H. Gao, Z. Cheng, W. Wu, A. Zhang, X. Chen, W. Wu, Y. Zhang, Usp5-rich apoptotic extracellular vesicles regulate nucleus pulposus cells apoptosis and DNA damage repair by preventing e2f1 proteasomal degradation, J Extracell Vesicles 14 (8) (2025) e70148.
15. J. Chen, T. Lin, Y. Yuan, P. Wu, S. Dai, H. Xu, J. Zhang, J. Ma, Comparative analysis of the immunomodulatory functions of dental follicle stem cells and their apoptotic vesicles, J. Stem Cells Regen. Med. 21 (1) (2025) 11–18.
16. M. Battistelli, and E. Falcieri, Apoptotic bodies: Particular extracellular vesicles involved in intercellular communication, Biology (Basel) 9 (1) (2020).

17. Y. Xia, J. Zhang, G. Liu, J. Wolfram, Immunogenicity of extracellular vesicles, Adv. Mater. 36 (33) (2024) e2403199.
18. X. Miao, X. Wu, W. You, K. He, C. Chen, J. L. Pathak, Q. Zhang, Tailoring of apoptotic bodies for diagnostic and therapeutic applications:Advances, challenges, and prospects, J. Transl. Med. 22 (1) (2024) 810.
19. R. Kalluri, The biology and function of extracellular vesicles in immune response and immunity, Immunity 57 (8) (2024) 1752–1768.
20. J. Chen, Z. Wang, S. Liu, R. Zhao, Q. Chen, X. Li, S. Zhang, J. Wang, Lymphocyte-derived engineered apoptotic bodies with inflammation regulation and cartilage affinity for osteoarthritis therapy, ACS nano 18 (43) (2024) 30084–30098.
21. Z. Li, Q. Cheng, L. Lin, X. Fu, Y. Wang, Plasma membrane-derived biomimetic apoptotic nanovesicles targeting inflammation and cartilage degeneration for osteoarthritis, Small Methods 9 (1) (2025) e2400660.
22. R. Wang, M. Hao, X. Kou, B. Sui, M. L. Sanmillan, X. Zhang, D. Liu, J. Tian, W. Yu, C. Chen, R. Yang, L. Sun, Y. Liu, C. Giraudo, D. A. Rao, N. Shen, S. Shi, Apoptotic vesicles ameliorate lupus and arthritis via phosphatidylserine-mediated modulation of t cell receptor signaling, Bioact. Mater. 25 (2023) 472–484.
23. H. Chen, S. Kasagi, C. Chia, D. Zhang, E. Tu, R. Wu, P. Zanvit, N. Goldberg, W. Jin, W. Chen, Extracellular vesicles from apoptotic cells promote tgfβ production in macrophages and suppress experimental colitis, Sci. Rep. 9 (1) (2019) 5875.
24. C. Carrasco-Padilla, O. Aguilar-Sopeña, A. Gómez-Morón, S. Alegre-Gómez, F. Sánchez-Madrid, N. B. Martín-Cófreces, P. Roda-Navarro, T cell activation and effector function in the human jurkat t cell model, Methods Cell Biol. 178 (2023) 25–41.
25. Q. Yang, W. Gao, X. Li, X. Li, X. Zhou, W. Li, C. Zhou, A. Luo, Z. Liu, Targeting abca1 via extracellular vesicle-encapsulated staurosporine as a therapeutic strategy to enhance radiosensitivity, Adv. Healthc. Mater. 13 (16) (2024) e2400381.
26. R. J. C. Bose, N. Tharmalingam, F. J. Garcia Marques, U. K. Sukumar, A. Natarajan, Y. Zeng, E. Robinson, A. Bermudez, E. Chang, F. Habte, S. J. Pitteri, J. R. McCarthy, S. S. Gambhir, T. F. Massoud, E. Mylonakis, R. Paulmurugan, Reconstructed apoptotic bodies as targeted "nano decoys" to treat intracellular bacterial infections within macrophages and cancer cells, ACS nano 14 (5) (2020) 5818–5835.
27. M. Prinz, S. Jung, J. Priller, Microglia biology: One century of evolving concepts, Cell 179 (2) (2019) 292–311.
28. L. Rao, S. Xia, W. Xu, R. Tian, G. Yu, C. Gu, P. Pan, Q. F. Meng, X. Cai, D. Qu, L. Lu, Y. Xie, S. Jiang, X. Chen, Decoy nanoparticles protect against covid-19 by concurrently adsorbing viruses and inflammatory cytokines, Proc. Natl. Acad. Sci. U. S. A. 117 (44) (2020) 27141–27147.
29. Z. Deng, T. Fan, C. Xiao, H. Tian, Y. Zheng, C. Li, J. He, Tgf-β signaling in health, disease and therapeutics, Signal transduction and targeted therapy 9 (1) (2024) 61.

30. X. Hu, W. Xu, Y. Ren, Z. Wang, X. He, R. Huang, B. Ma, J. Zhao, R. Zhu, L. Cheng, Spinal cord injury: Molecular mechanisms and therapeutic interventions, Signal transduction and targeted therapy 8 (1) (2023) 245.
31. F. H. Brennan, Y. Li, C. Wang, A. Ma, Q. Guo, Y. Li, N. Pukos, W. A. Campbell, K. G. Witcher, Z. Guan, K. A. Kigerl, J. C. E. Hall, J. P. Godbout, A. J. Fischer, D. M. McTigue, Z. He, Q. Ma, P. G. Popovich, Microglia coordinate cellular interactions during spinal cord repair in mice, Nature Communications 13 (1) (2022) 4096.
32. X. Xue, X. Wu, Y. Fan, S. Han, H. Zhang, Y. Sun, Y. Yin, M. Yin, B. Chen, Z. Sun, S. Zhao, Q. Zhang, W. Liu, J. Zhang, J. Li, Y. Shi, Z. Xiao, J. Dai, Y. Zhao, Heterogeneous fibroblasts contribute to fibrotic scar formation after spinal cord injury in mice and monkeys, Nature Communications 15 (1) (2024) 6321.
33. Y. Rong, J. Wang, T. Hu, Z. Shi, C. Lang, W. Liu, W. Cai, Y. Sun, F. Zhang, W. Zhang, Ginsenoside rg1 regulates immune microenvironment and neurological recovery after spinal cord injury through mycbp2 delivery via neuronal cell-derived extracellular vesicles, Adv. Sci. 11 (31) (2024) e2402114.
34. S. Han, D. Zhang, Y. Kao, X. Zhou, X. Guo, W. Zhang, M. Liu, H. Chen, X. Kong, Z. Wei, H. Liu, S. Feng, Trojan horse strategy for wireless electrical stimulation-induced zn(2+) release to regulate neural stem cell differentiation for spinal cord injury repair, ACS nano 18 (47) (2024) 32517–32533.
35. L. Wang, H. Zhao, M. Han, H. Yang, M. Lei, W. Wang, K. Li, Y. Li, Y. Sang, T. Xin, H. Liu, J. Qiu, Electromagnetic cellularized patch with wirelessly electrical stimulation for promoting neuronal differentiation and spinal cord injury repair, Adv. Sci. 11 (30) (2024) e2307527.
36. J. Cao, X. Zhang, J. Guo, J. Wu, L. Lin, X. Lin, J. Mu, T. Huang, M. Zhu, L. Ma, W. Zhou, X. Jiang, X. Wang, S. Feng, Z. Gu, J. Q. Gao, An engineering-reinforced extracellular vesicle-integrated hydrogel with an ros-responsive release pattern mitigates spinal cord injury, Sci Adv 11 (14) (2025) eads3398.

Figures

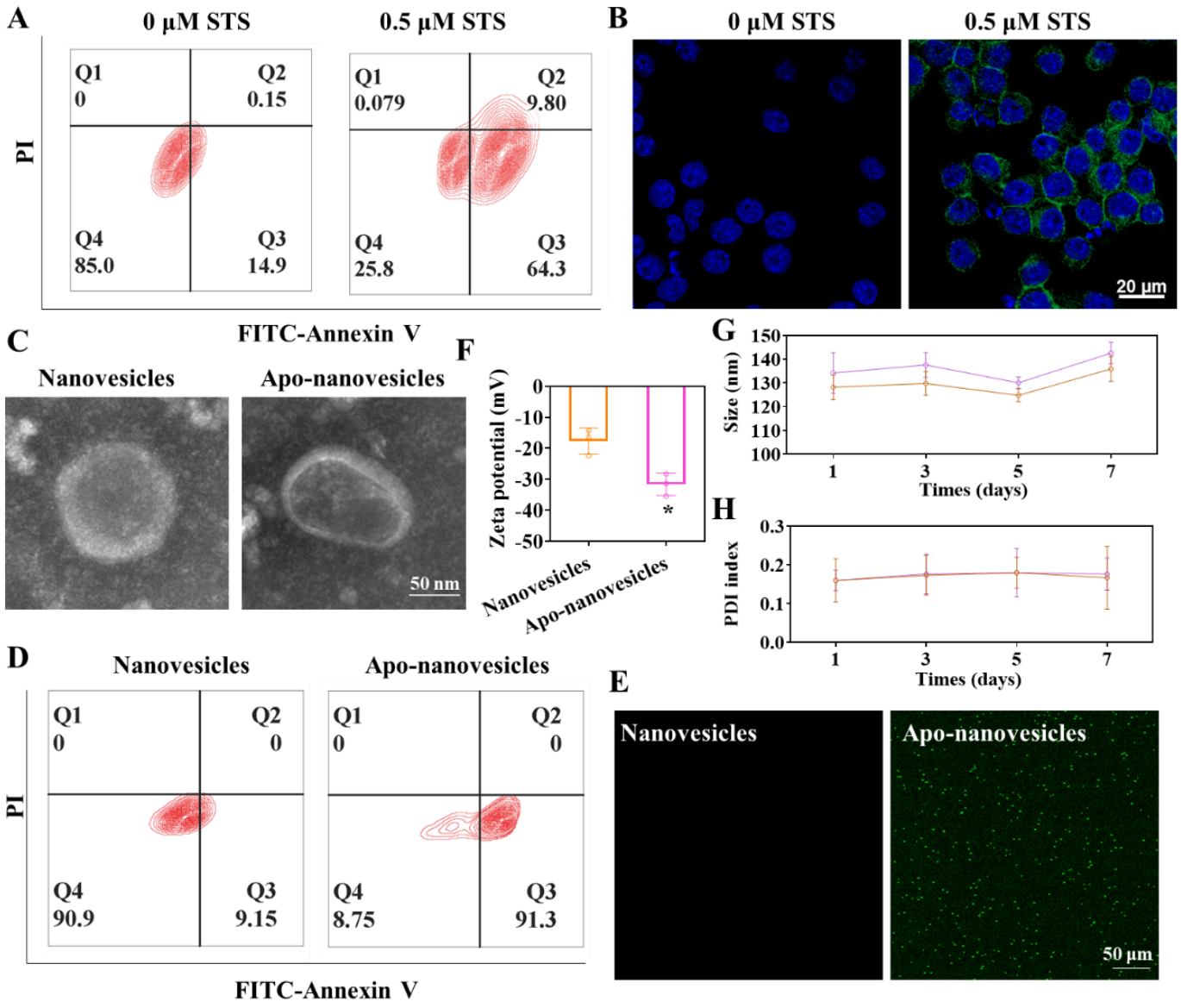


Figure 1

Characterization of Apo-nanovesicles derived from early apoptotic Jurkat T cells. (A) Flow cytometric quantification of apoptosis in Jurkat cells stained with Annexin V-FITC and PI. (B) Fluorescence microscopy images of apoptotic Jurkat cells. (C) Representative transmission electron micrographs showing the cup-shaped morphology of both control nanovesicles and Apo-nanovesicles. (D) Flow cytometric detection of phosphatidylserine exposure via FITC-Annexin V binding to Apo-nanovesicles. (E) Fluorescent staining of Apo-nanovesicles with Annexin V-FITC confirming surface phosphatidylserine presentation. (F) Zeta potential measurements comparing the surface charge of nanovesicles and Apo-nanovesicles (n = 3; *p < 0.05). (G) Hydrodynamic size distribution of Apo-nanovesicles assessed by DLS. (H) PDI of Apo-nanovesicles determined via DLS.

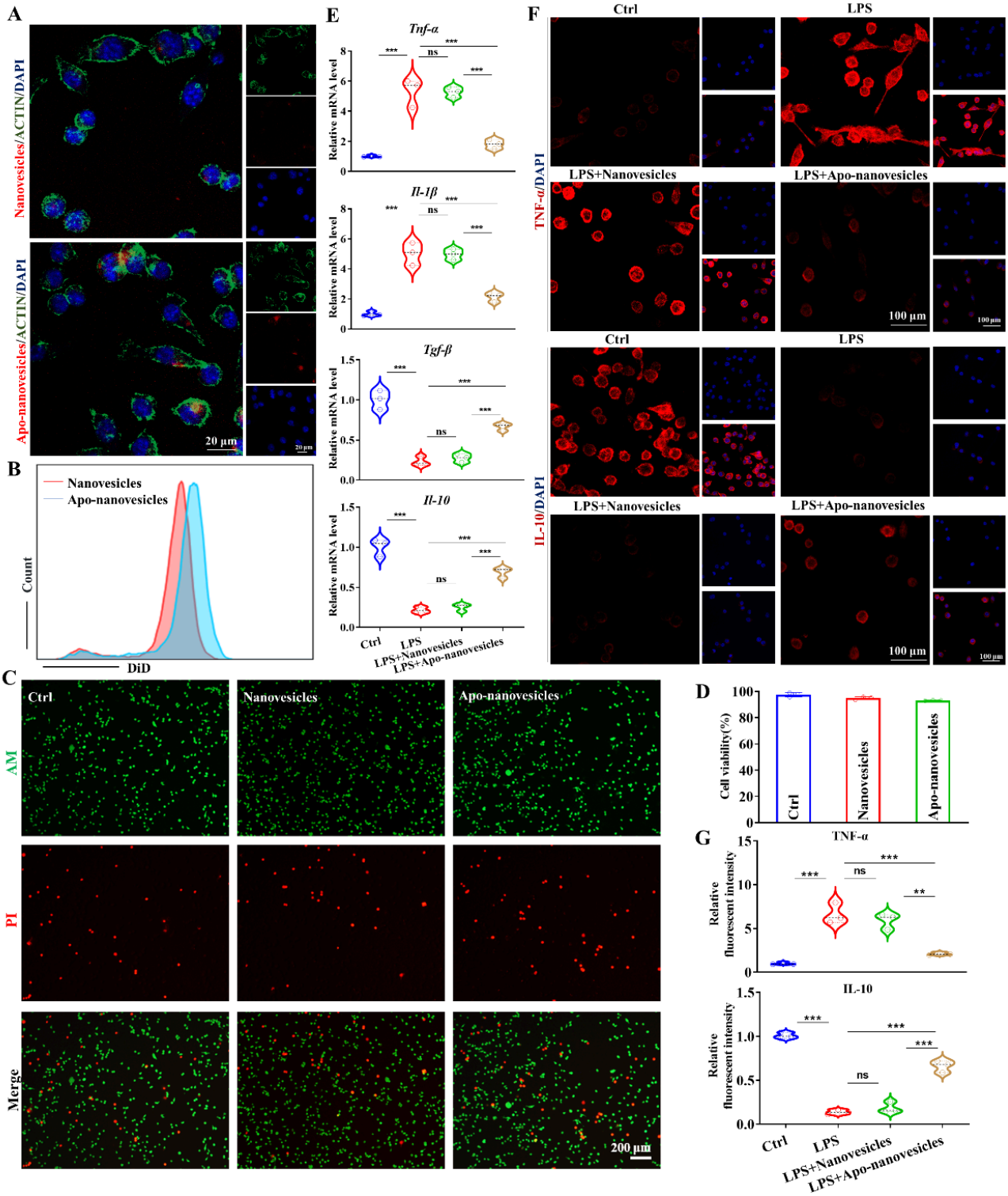


Figure 2

Immunomodulatory properties of Apo-nanovesicles on microglial polarization. (A)Confocal laser scanning microscopy images illustrating cellular internalization of DiD-labeled Apo-nanovesicles (red). Cytoskeletal F-actin and nuclei were counterstained with phalloidin (green) and DAPI (blue), respectively. (B) Flow cytometry analysis of microglial phagocytosed with nanovesicles. (C) Live/Dead staining (green: calcein AM, live cells; red: PI, dead cells) of microglial after 72 h exposure to nanovesicles or Apo-

nanovesicles. (D) Viability of microglia after treatment with nanovesicles or Apo-nanovesicles, evaluated by CCK-8 assay. (E) Quantitative PCR analysis of key M1 and M2 phenotypic markers. (F) Immunofluorescence staining of the pro-inflammatory cytokine TNF-α and the anti-inflammatory cytokine IL-10. (G) Quantitative analysis of TNF-α and IL-10 in Figure 2 F. Data represent mean ± SD (n = 3; ***p < 0.001, **p < 0.01, *p < 0.05; ns, not significant).

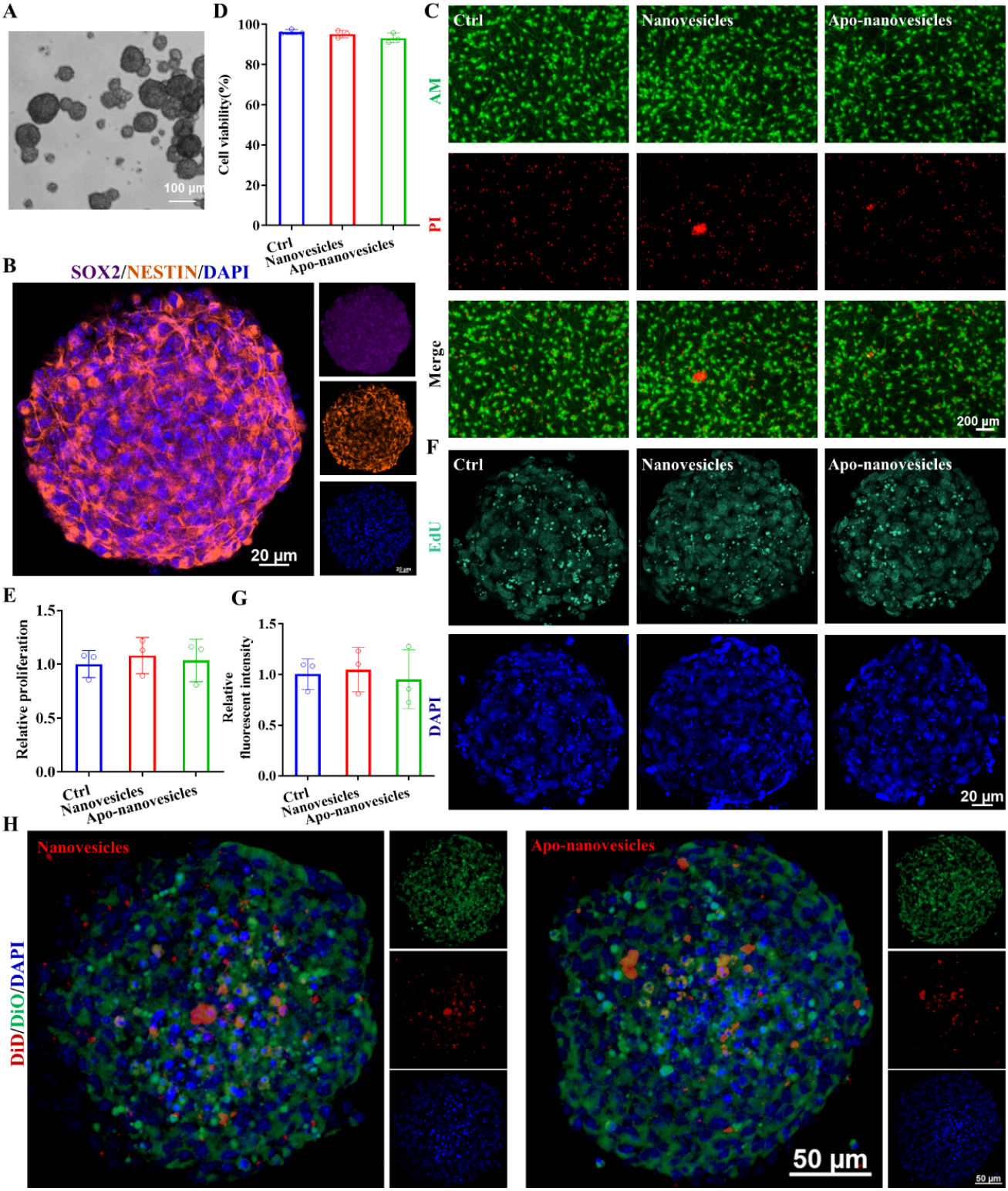


Figure 3

Biocompatibility evaluation of Apo-nanovesicles with neural stem cells. (A) Representative bright-field image of neurospheres formed by mNSCs. (B) Immunofluorescence analysis of stemness markers SOX2 and NESTIN. (C) Viability of NSCs after 72 h exposure to Apo-nanovesicles assessed by Live/Dead staining. (D) Quantitative assessment of cell viability from (C). (E) Proliferation of NSCs measured via CCK-8 assay. (F) EdU incorporation assay evaluating NSCs proliferative activity. (G) Quantitative analysis of EdU fluorescence intensity. (H) Cellular internalization of DiD-labeled nanovesicles (red). Cell membranes and nuclei were stained with DiO (green) and DAPI (blue), respectively.

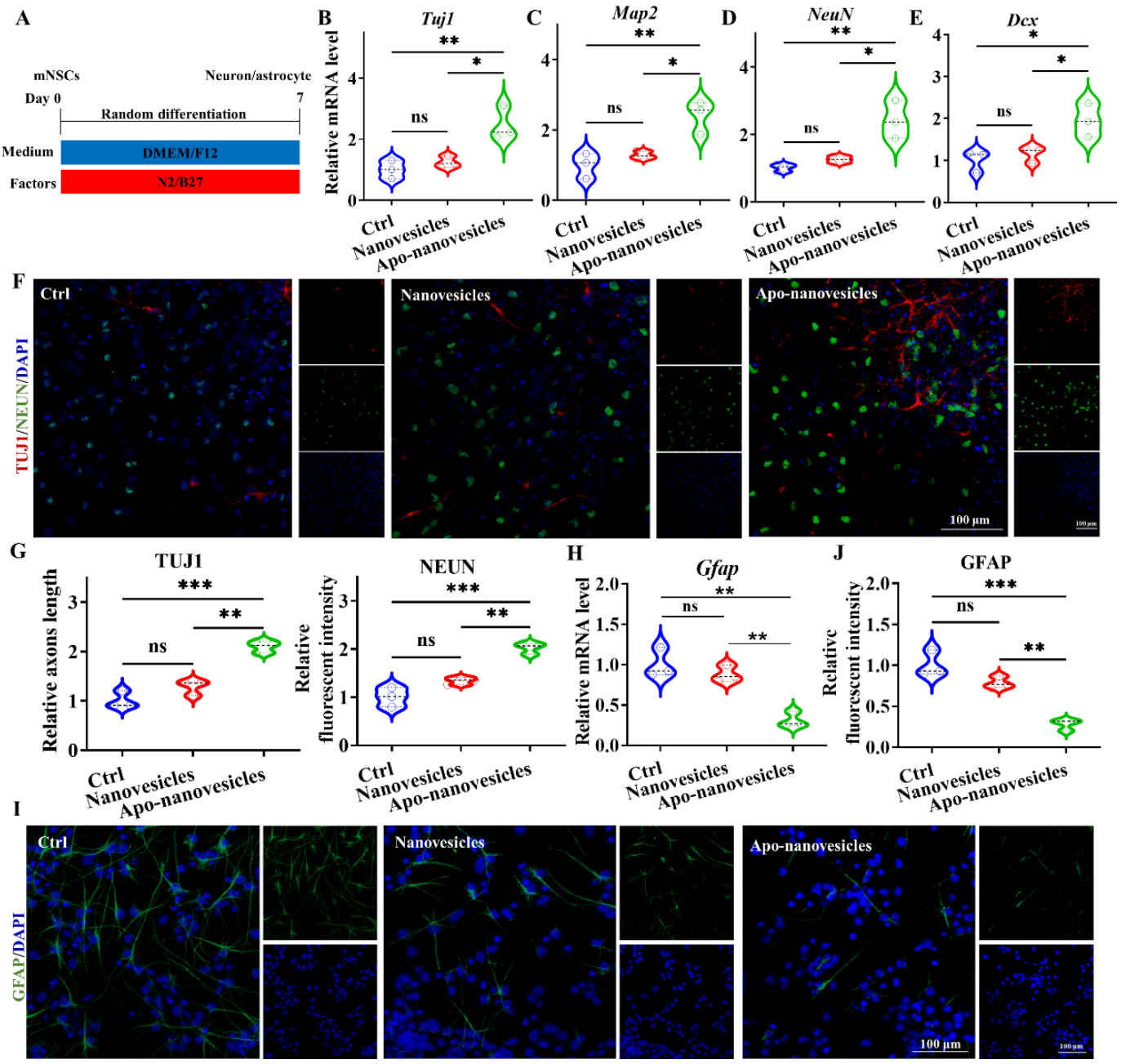


Figure 4

Promotion of neuronal differentiation in NSCs treated with Apo-nanovesicles. (A) Schematic diagram of the 7-day spontaneous differentiation protocol. (B–E, H) qPCR analysis of neuronal markers (*Tuj1, NeuN, Map2, Dcx*) and the astrocytic marker *Gfap*. (F, I) Immunofluorescence staining for TUJ1, NEUN, and GFAP proteins. (G, J) Quantification of relative expression for TUJ1, NEUN, and GFAP from Figs. 4F, I. All data are presented as mean ± SD (n = 3; ***p < 0.001, **p < 0.01, *p < 0.05; ns, not significant).

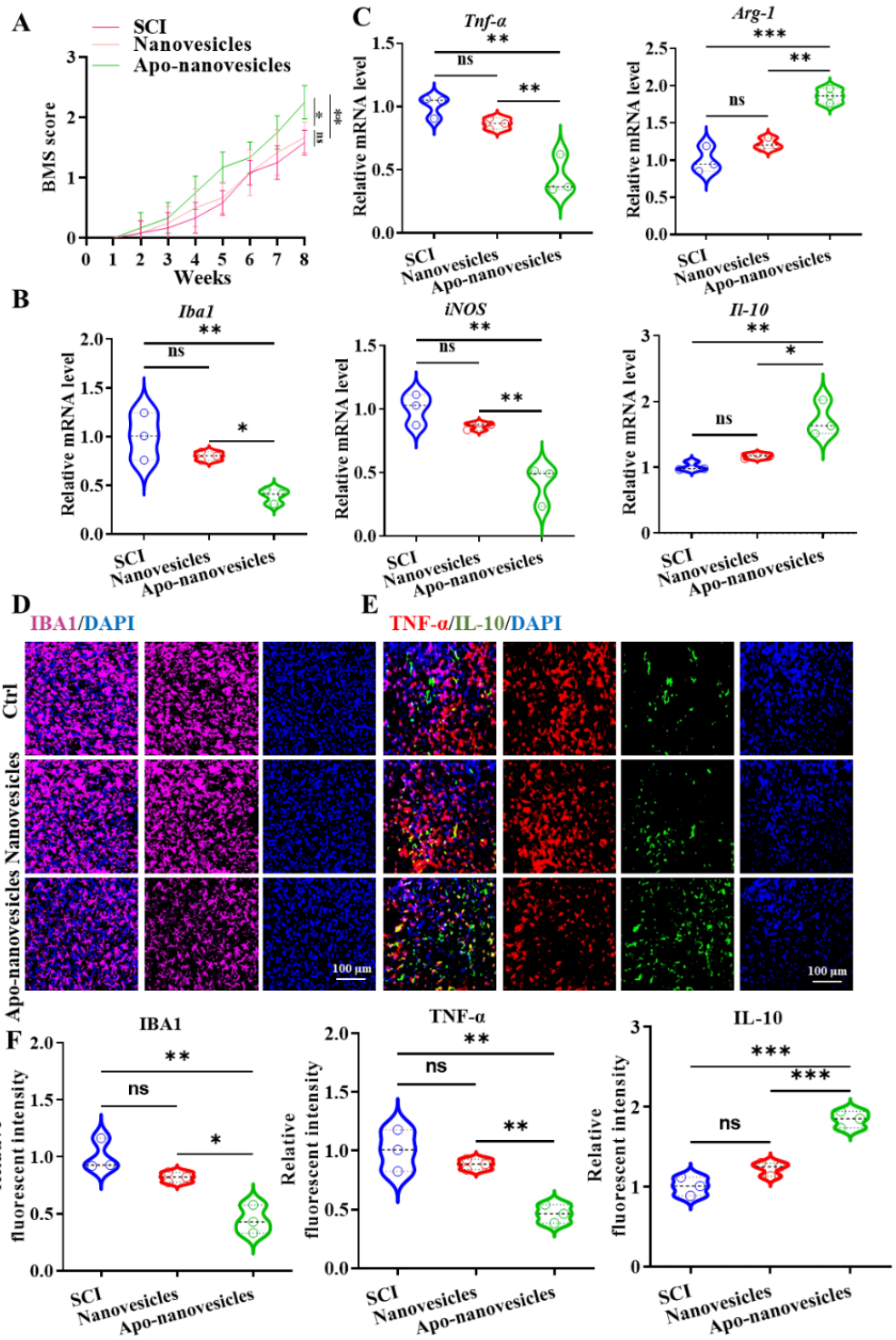


Figure 5

Therapeutic efficacy of Apo-nanovesicles in a murine spinal cord injury model. (A) Time-dependent functional recovery assessed by Basso Mouse Scale scoring over 8 weeks. (B, C) qPCR analysis of microglial and inflammatory markers. (D, E) Immunofluorescence staining of IBA1, TNF-α, and IL-10. (F) Quantification of relative fluorescence intensity for IBA1, TNF-α, and IL-10 from Figs. 5D, E. Values are mean ± SD (n = 3; ***p < 0.001, **p < 0.01, *p < 0.05; ns, not significant).

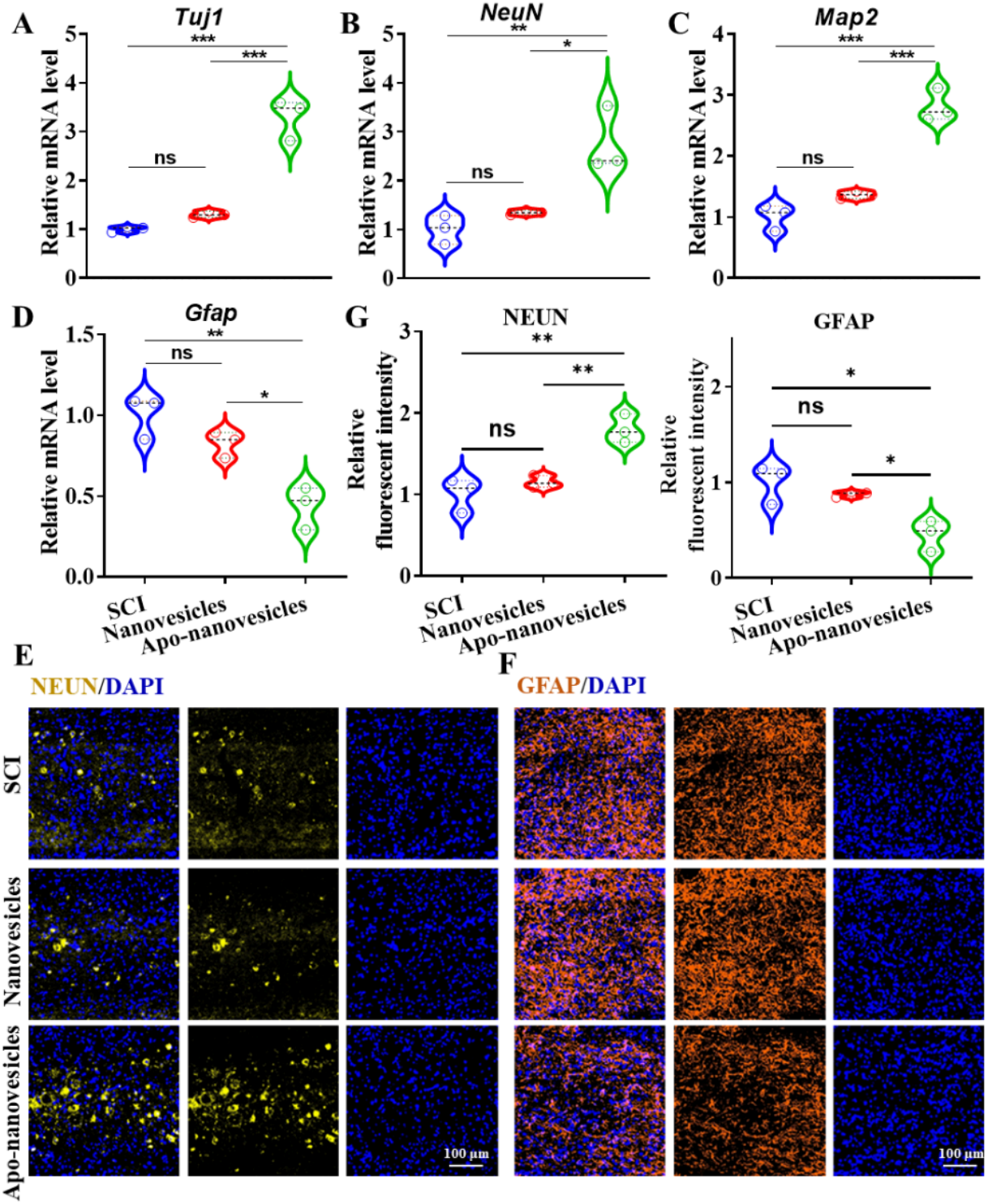


Figure 6

Modulation of nerve regeneration by Apo-nanovesicles post-SCI. (A–D) qPCR evaluation of neural and glial gene expression in spinal cord tissues. (E, F) Representative immunofluorescence images of neurons and astrocytes. (G) Quantitative analysis of immunofluorescence intensity for NEUN and GFAP from Figs. 6E, F. Data represent mean ± SD (n = 3; ***p < 0.001, **p < 0.01, *p < 0.05; ns, not significant).

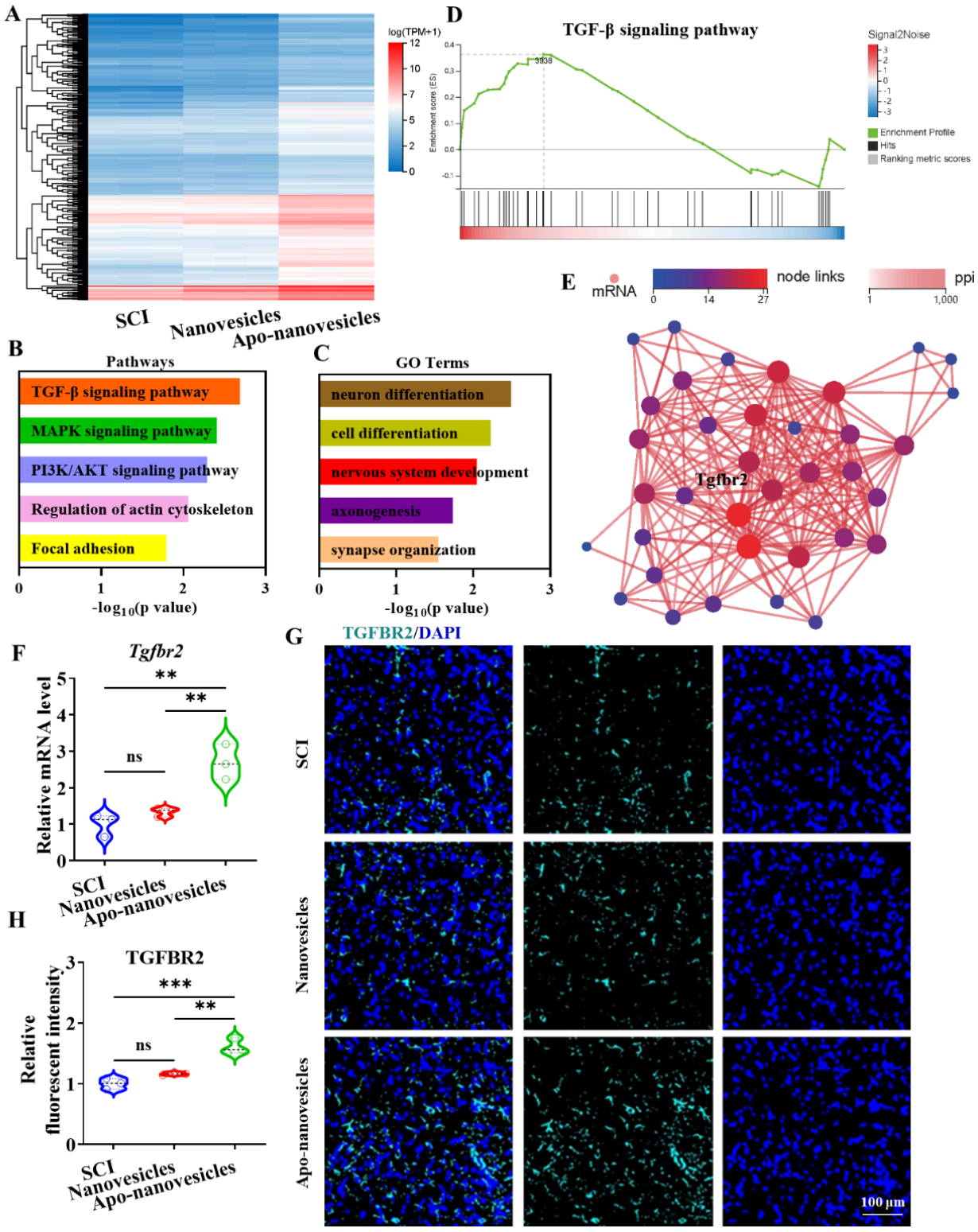


Figure 7

Transcriptomic profiling of spinal cord tissue. (A) Heatmap of DEGs. (B) KEGG pathway enrichment analysis of DEGs. (C) GO enrichment analysis. (D) Gene set enrichment analysis (GSEA) of the TGF-β signaling pathways. (E) Protein–protein interaction (PPI) network of key DEGs. (F) qPCR validation of *Tgfbr2*. (G, H) Representative immunofluorescence images and quantitative analysis of immunofluorescence intensity for TGFBR2. Data represent mean ± SD (n = 3; ***p < 0.001, **p < 0.01; ns, not significant).

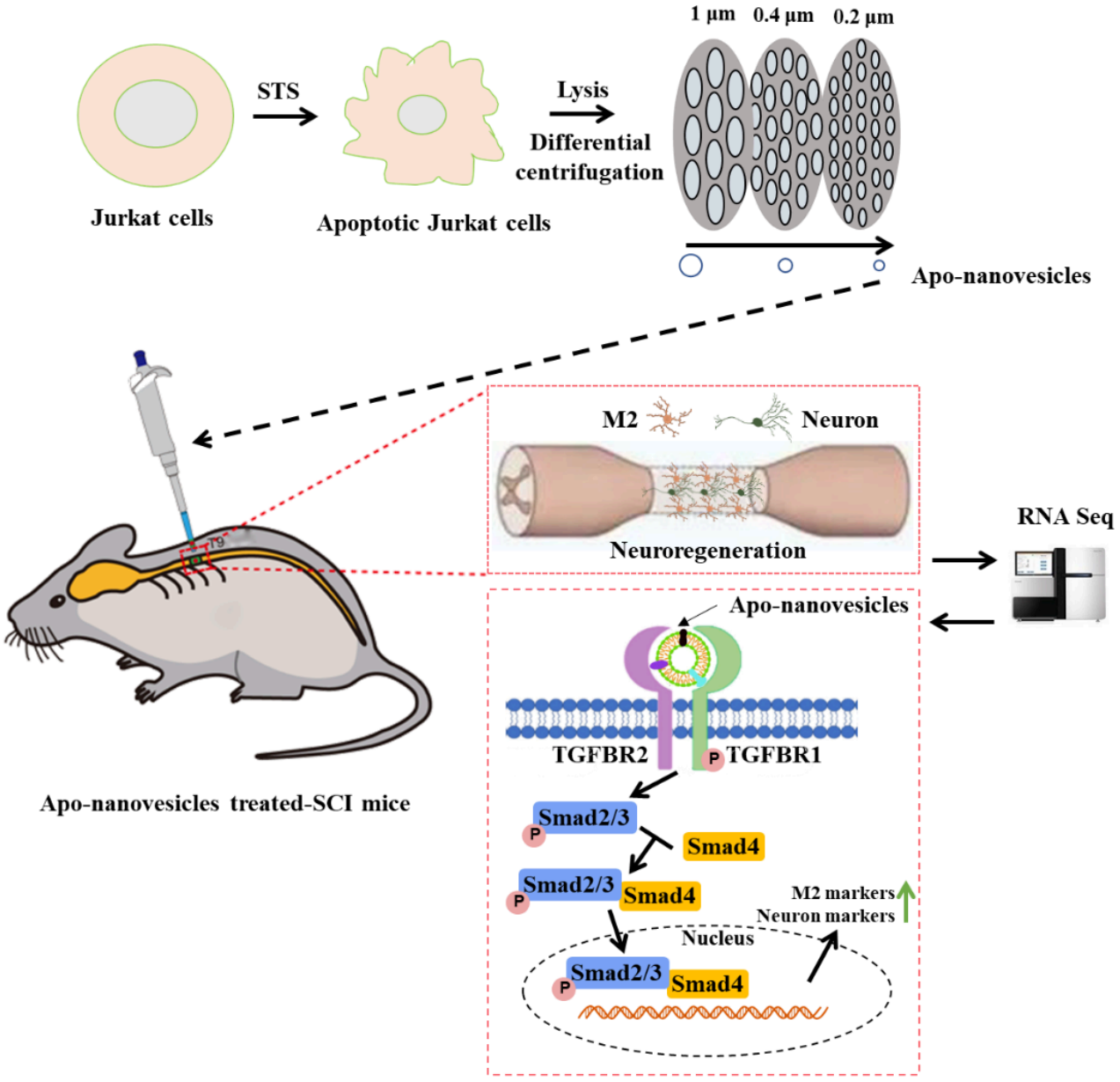


Figure 8

Schematic diagram of the repair of SCI by Apo-nanovesicles.

Supplementary Files

This is a list of supplementary files associated with this preprint. Click to download.

- SupplementaryMaterial.docx